6th INTERNATIONAL SCIENTIFIC CONFERENCE
ON DEFENSIVE TECHNOLOGIES
OTEH 2014
Belgrade, Serbia, 9 – 10 October 2014

DISCRETIZATION OF THE FINITE ELEMENT NETWORK ALONG THE CRACK LINE IN THE CONCRETE

EDVIN BOLIĆ
University in Bihać – Faculty of Technical Engineering Bihać, Bihać, edvinbolic@hotmail.com

DŽENANA GAČO
University in Bihać – Faculty of Technical Engineering Bihać, Bihać, dzgaco@bih.net.ba

FADIL ISLAMOVIĆ
University in Bihać – Faculty of Technical Engineering Bihać, Bihać, f.islam@bih.net.ba

MERSIDA MANJGO
University in Mostar – Faculty of Mechanical Engineering, Mostar, mersida.manjgo@unmo.ba

Abstract: *The fracture mechanics of concrete is connected to two things that are regularly subject to research: the length of the fracture process zone (FPZ) and the width of the fracture process zone (FPZ). Following the examination of this problem, this paper describes the process of discretization of the crack in the concrete using finite element method and its application for the determination of concrete fracture mechanics parameters. The results of testing on concrete samples made of concrete grade C30/37 of river gravel and crushed stone were processed. The paper demonstrates the principle of modeling such problems.*

Keywords: *concrete, fracture mechanics, fracture parameters, crack length, linear elastic fracture mechanics (LEFM) , non-linear fracture mechanics (NFM) , fracture process zone (FPZ) , finite element method (FEM).*

1. INTRODUCTION

Concrete structures are full of damages that occur due to the hydration process, during strengthening and load application in the exploitation process.

These are the damages that occur in the form of micro cracks which can gradually grow to considerable size and cause problems in structure exploitation or even lead to its failure.

For these reasons, fracture mechanics of concrete structures that treat these issues significantly helps in observing occurrence of these processes in the concrete structures.

The area, located in front of the macro crack, is called fracture process zone (FPZ) in the concrete. In the fracture process zone (FPZ) concrete still has the ability to transmit stress, i.e. it has defined remaining strength.

This paper describes the modeling fracture areas process in the concrete directly in the fracture process zone (FPZ).

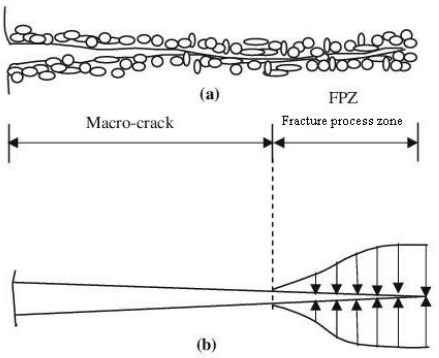

Figure 1. (a) Fracture process zone in the concrete;
(b) Distribution of cohesive stress in FPZ

This paper we will try to define how to model the fracture zone in the concrete directly in the fracture process zone (FPZ).

2. DISCRETIZATION WITH THE FINITE ELEMENT METHOD

There are two values in fracture mechanics that regularly provoke the interest of scientists in the field of fracture modeling in the concrete, and that are (i) the fracture process zone (FPZ), and (ii) the width of the fracture process zone

The experimental testing conducted by Peterson (1981) show that the length of the FPZ (fracture process zone) is significant and comparable, and the width is usually small compared to the length (depending on the maximum size of the agregate) and compared to the structure size.

The most commonly used models are effective crack model (ECM) and cohesive crack model (CCM), which begin with the assumption that the fracture process zone (FPZ) is reduced to a line in a one-dimensional analysis or to a surface in a two-dimensional analysis.

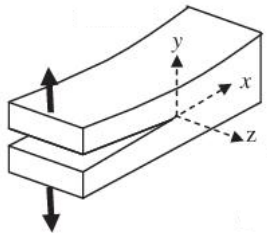

Figure 2. Model I of crack opening (split tension)

When one macroscopic crack opens inside the defined direction for the clean Model I (Figure 2), cohesive crack can be easily modeled by means of the procedures proposed by Petersson (1981), which were further improved by Carpinteri (1989) and Planas and Elices (1991).

In this model, the number of nodes along the potential fracture line is retained as fixed in the standard linear elastic finite element method (FEM).

The potential fracture line for TPBT sample is shown in Figure 3. In the case of application of finite element method, the nodes in the crack are arranged so that the first is at the bottom of the crack, and n is at the tip of the crack along the potential fracture line.

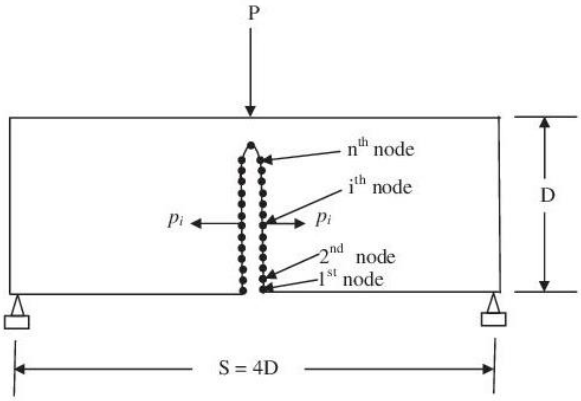

Figure 3. Discretization of finite elements along the fracture line

Crack opening along the fracture line is caused by external load acting on the structure and grouped in the column *w* matrix and corresponding force on the nodes which are located in the column *F* matrix.

The remaining node displacements and forces in the nodes for the remaining part of the structure are grouped in a column w_R and F_R matrix. This matrix form can be described as follows:

$$\begin{Bmatrix} F \\ F_R \end{Bmatrix} = -\begin{bmatrix} K_{CC} & K_{CR} \\ K_{RC} & K_{RR} \end{bmatrix} \begin{Bmatrix} w \\ w_R \end{Bmatrix} \quad (1)$$

If we say that there are no other forces that affect the remainder of the sample, $[F_R]$=0, and exclude all components of displacement w_R from the expression, the matrix form of balance equation would have the following form:

$$\{F\} = [K_F]\{w\} \quad (2)$$

where:

$$[K_F] = [K_{CC}] - [K_{CR}][K_{RR}]^{-1}[K_{RC}] \quad (3)$$

Crack opening for *n* nodes along the fracture zone is expressed in the following adjusted expression:

$$\{w\} = [K]\{p\} + \{C\}P + \{P_g\} \quad (4)$$

In this equation $\{w\}$ is the vector that represents the movement of nodes on the crack, $[K]$ is the symmetric matrix and K_{ij} members represent crack opening in the node *i*, initiated by unit tensile force which causes the crack opening and is applied at node *j*, $\{p\}$ is the load vector in the nodes, $\{C\}$ is vector that represents the value of crack opening in the node and when P=1 (unit value). Finally,$\{p_g\}$ is crack opening vector in the point and the sample weight.

In this analysis, we improved the methods of influence by Planas and Elices (1991), who used it to solve the equations (4). Assuming that the total number of nodes on the crack line is n and that the initial crack tip lies on the k-node, based on this method, the equation (4) is thickened between nodes *i=1,2,3,.....(k-1)* in the nodes *i=k,(k+1),(k+2),.....,n*. The equation (4) can now be written as follows:

$$\begin{Bmatrix} w_N \\ w_L \end{Bmatrix} = \begin{bmatrix} K_{NN} & K_{NL} \\ K_{LN} & K_{LL} \end{bmatrix} \begin{Bmatrix} p_N \\ p_L \end{Bmatrix} + \begin{Bmatrix} C_N \\ C_L \end{Bmatrix} P + \begin{Bmatrix} p_{gN} \\ p_{gL} \end{Bmatrix} \quad (5)$$

Indexes *N* and *L* mark a part of the notch for *i = 1,2,....,(k-1)* and inter zones *i=k,(k+1),(k+2),...,n*. Since the crack opening width in the zone where *i=k,(k+1),(k+2),...,n* equals to zero, the initial crack in that zone without tensile strength can be express as follows:

$$\begin{matrix} \{p_N\} = \{0\}, \ za\ i = 1,2,3, \dots\dots\dots\dots, (k-1) \} \\ \{w_L\} = \{0\}, \ za\ i = k, (k+1), (k+2), \dots, n \} \end{matrix} \quad (6)$$

Expressions (5) and (6) become:

$$\{p_L\} = [M_{LL}]\{w_L\} - [M_{LL}]\{C_L\}P - [M_{LL}]\{P_{gL}\} \quad (7)$$

where:

$$M_{LL} = K_{LL}^{-1}, \{T_L\} = [M_{LL}]\{C_L\}, \{T_g\} = [M_{LL}]\{P_{gL}\}$$

$$\{p_L\} = [M_{LL}]\{w_L\} - \{T_L\}P - \{T_g\} \quad (8)$$

Furthermore, this binding area can be divided between cohesive (damaged) zone and non-cracked (undamaged) zone along the fracture line. If we consider that cohesive zone between nodes is *j=k,(k+1),....,l* and undamaged part of *j=(l+1),(l+2),...,n*, then with further thickening in the equation (8) we can write the following expression:

$$\begin{Bmatrix} P_{LC} \\ P_{LU} \end{Bmatrix} = \begin{bmatrix} M_{LLCC} & M_{LLCU} \\ M_{LLUC} & M_{LLUU} \end{bmatrix} \begin{Bmatrix} W_{LC} \\ W_{LU} \end{Bmatrix} - \begin{Bmatrix} T_{LC} \\ T_{LU} \end{Bmatrix} P - \begin{Bmatrix} T_{gC} \\ T_{gU} \end{Bmatrix} \quad (9)$$

In the above expression indexes C and U denote the cohesive zones for *j=k,(k+1),.....l* and undamaged zone for *j=(l+1), (l+2),....,n*. The width of the crack opening in the undamaged zone and in the last point of the cohesive zone is equal to zero, which can mathematically be expressed as:

$$\{w_{LU}\} = 0, \ \{w_{LC}\}_{j=l} = 0 \quad (10)$$

Equations (9) and (10) become:

$$\{p_{LC}\} = [M_{LLCC}]\{w_{LC}\} - \{T_{LC}\}P - \{T_{gC}\} \quad (11)$$

For *j=l* node applied load can be expressed follows:

$$P = \frac{\sum_{j=k}^{l-1}\{M_{LLCC}\}_{l,j}\{W_{LC}\}_j - \{P_{LC}\}_{j=l} - \{T_gC\}_{j=l}}{\{T_{LC}\}_{j=l}} \quad (12)$$

With equations (11) and (12) for nodes *j=k, (k+1), (k+2),.....,(l-1)* a large number of non-linear dependent equations can be formed for crack opening in the cohesive zone.

Functional form of non-linear dependent equations can be expressed as:

$$\{Z\} = [M_{LLCC}]\{W_{LC}\} - \{P_{LC}\} - \{T_{LC}\} \cdot \cdot \frac{\sum_{j=k}^{l-1}\{M_{LLCC}\}_{l,j}\{W_{LC}\}_j - \{P_{LC}\}_{j=l} - \{T_gC\}_{j=l}}{\{T_{LC}\}_{j=l}} - \{T_{gC}\} \quad (13)$$

If sign convention is used properly, this can be written as

$\{p_{LC}\} = -F_{uc}f(w_{LC})$, where in order to have proper discretization, we conduct division on the network size h, $F_{uc} = Bhf_t$, for all values i except for the value of *i=k*, and *i=n*; and $F_{uc} = Bhf_t/2$ for *i=k* and *i=n*. The solution to the equation (13) is obtained by using the Newton-Rapshon method.

Function Z and its Jacobian matrix for unknown crack opening (displacement) use different softening functions which are programed in separate functions.

Thus, this method becomes useful and effective as well as many types of softening rules as much as they can be incorporated into the program.

Following the solutions of the equation (13) for $\{w_{LC}\}$, the value of P can be determined with the equation (12) and the value $\{p_{LC}\}$ with the equation (11). Returning backwards to equation (10), (9), (8), (6), (5) and (4) it is possible to determine all of the unknown values for $\{w\}$ and $\{p\}$.

3.DETERMINING THE DEFLECTION ON THE BEAM

For known values of parameters $\{p\}$ and P, deflection in the middle of the beam δ is determined according to the following expression:

$$\delta = D_L P + \{D_p\}^T\{p\} + D_g \quad (14)$$

D_L is deflection in the point where the load acts when the external load is P = 1 (unit), $\{D_p\}$ the load vector at the point of deflection when the vector unit load is $\{p\} = \{1\}$, D_g presents a deflection in the middle of the beam due to its own sample weight.

Members $[K], \{C\}, \{p_g\}$, and D_g in the formulas (4) and (14) can be calculated using standard linear elastic finite element method.

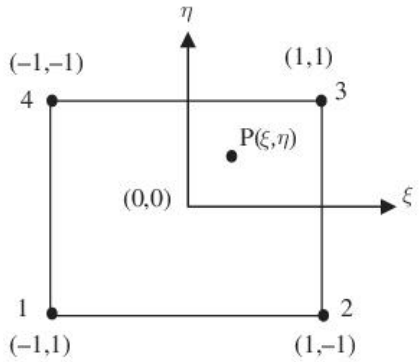

Figure 4. Typical four-node isoparametric plane element in (ξ,η) coordinates

Experiments were conducted so that the finite element network in bands 3D/4 and D varies, whereas in the band of D/4 width is retained in the same ratio (aspect ratio of square sides in finite element network is equal to 1). The experimental testing was conducted on samples with dimensions B=100[mm], D= 100 [mm] and S = 400[mm].

The characteristic values of the used material are determined with WST test on standard concrete cylinder (150mm x 300mm).

The resulting material properties have the following values : ν= 0,10, E=36,5 [GPa], f_t=3,29 [MPa], and G_F=110 [N/m]. All beams are made of constant dimension and the height of the sample is D = 100[mm]. Notch on the beam was taken in ratio of 1/3 notch to beam height a_0/D.

The test results conducted on the beam samples in the laboratory are shown in Table 1.

Table 1: Test results of three-point bending geometry for notched concrete beam

D (mm)	Sample	S (mm)	a_0 (mm)	P (kN)	σ_{Nu} (MPa)	G_F (N/m)
	B100-k1			6,321	2,71	118
100	B100-k2	400	33	6,124	2,67	113
	B100-k3			6,028	2,61	109
	B100-r1			5,362	2,45	106
100	B100-r2	400	33	5,089	2,19	101
	B100-r3			5,158	2,32	104

Finite element network was selected so that the sample was divided into 16 equal parts by height D.

In the longitudinal direction the division was conducted so that the band D/2 was divided to 8 parts, band 3D/4 to 8 parts and band D to four equal parts. A total of 14 nodes were selected along the fracture line.

4. EXPERIMENTAL PART OF THE PAPER

4.1 Description of the samples and models

In this example we consider the sample of the notched beam, which was used for further testing, and the sample was examined according to the below specified geometric relationships.

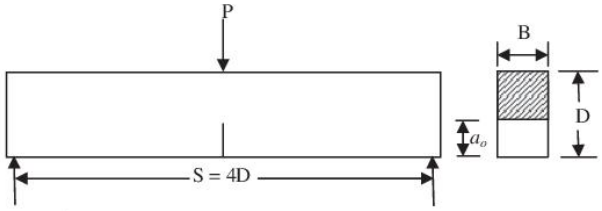

Figure 5. Geometry of test sample of notched beam

Discretization of the beam by the finite elements was conducted as shown in Figure 6.

Discretization of the beam was performed with typical four-sided isoparametric elements with four nodes, as shown in Figure 4.

In order to simplify the calculation beam was divided by its length in the areas D; 3D/4, D/2, 3D/4 and finally D.

According to this division we have the middle (D/2) width band, which was divided using finite elements network, and the remaining bands along the tested beam of 3/4D and D width, whose division was conducted on a smaller number of finite elements.

Discretization of the beam by height D was conducted so that the number of divisions in the D/2 width band was selected and the aspect ratio of square sides in finite element network is equal to 1.

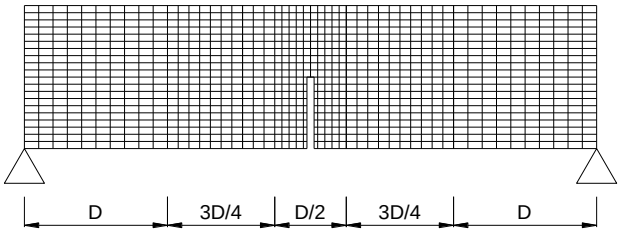

Figure 6. Method of forming a finite element network

In each case, finite element network can be selected and thickened in a different method, depending on the computer's memory.

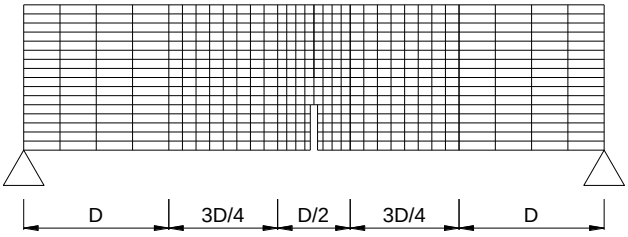

Figure 7. Method of forming a 512 finite elements network on a sample

As can be seen in Figure 7, a network of 512 finite elements was adopted, the number of degrees of freedom is 561, and the number of nodes along the potential fracture line is 14.

Firstly, coefficients such as $[K]$,$\{C\}$,$\{p_g\}$, $\{D_p\}$, D_L and D_g were obtained by the linear elastic finite element method.

These coefficients are determined once during the experiment and are used all the time in determining the cohesive crack propagation. In the beginning, while the state in the element is linear elastic, tensile stress in the k node will reach the limit of concrete tensile stress, and formation of crack will first occur in this node.

After that cohesive forces in the material begin to act on neighboring nodes according to given softening law. At this time the unknown values are $\{w_{LC}\}_{j=k}$, $(k+1), \dots, (l-1)$and P, and are determined with equations (12) and (13). Subsequently, the values $\{w\}$ and $\{p\}$are calculated, and then the beam deflections δ are determined using equation (14).

In this step, the first point of the P-CMOD and curve that shows the relationship between load and strain (P-δ) are determined. In the second phase of the calculation, external load P was increased to the value where the tensile stress in the concrete at the node (k +1) is greater than the strength of concrete in tension.

At this point we now have a situation that crack is formed in the node (k+1) with cohesive forces acting in that node. In the same manner, as mentioned above in second phase, the values of P-CMOD and P-δ curve are calculated.

This process continues until the crack develops in the node (l-1), and continues until the crack reaches node l=n.

The number of unknown values in each step is as high as the number of nodes where crack occurred in the cohesive zone.

At each stage of the calculation, the value of COD (crack opening displacement) is checked and when it becomes greater than or equal to w_c (max. COD) corresponding values of forces in the nodes take the value zero.

This same calculation is conducted on a sample with thicker finite elements network. 30 finite elements were selectedby height, band D was divided to 10 parts, band 3D/4 also to 10 equal parts and band D/2 to 15 equal parts.

In this case we got a network of 1650 finite elements, the number of degrees of freedom is 1736, and the number of nodes along the potential fracture line is 20.

Peak loads obtained from the numerical results for the first case is 7.15 kN and for the second case of division to the thicker finite element network is 6.71 kN.

5. CONCLUSION

It has been determined through these examples that the finite element network in these cases did not much affect the coefficients along the fracture lines. It was shown that even if we make the relatively thicker finite element network such model provides stable peak load values for these samples.

REFERENCES

[1] Shailendra Kumar, Sudhirkumar V. Barai, *Concrete Fracture Models and Applications*, Springer –Verlag Berlin Hridelberg 2011.

[2] H. Mihashi, K Rokugo, *ConcreteFracture Mechanics of Concrete Structures, Volume II*, AEDIFICATIO Publishers 1998.

[3] Carpinteri A, Columbo G, *Concrete Numerical analysis of catastrophic softening behaviour (snap-back instability)*, AEDIFICATIO Department of Structural Engineering, Politecnico di Torino, Italy ENEL-CRIS, 20162 Milano, Italy 1989.